Correlation between anomalous hydrogen absorption and ^{56}Fe-bonding strength in the $Zr(Al_xFe_{1-x})_2$ system

A. Israel and I. Jacob
Department of Nuclear Engineering, Ben-Gurion University of the Negev, Beer Sheva 84105, Israel

R. Moreh
Nuclear Research Center–Negev, Beer Sheva 84190, Israel
and Department of Physics, Ben-Gurion University of the Negev, Beer Sheva 84105, Israel

O. Shahal, A. Wolf, and M. Fogel
Nuclear Research Center–Negev, Beer Sheva 84190, Israel
(Received 28 December 1993; revised manuscript received 21 March 1994)

The nuclear-resonant-photon-scattering technique was utilized to monitor the iron binding properties in the intermetallic $Zr(Al_xFe_{1-x})_2$ system. The ^{56}Fe isotope scatters elastically 8.512-MeV γ rays emitted by a $Cr(n,\gamma)$ source. An experimental comparison of the scattered intensity from the different compounds reflects the corresponding variation of the iron cohesion properties. The experimental results were quantified by evaluating the mean vibrational kinetic energies or effective temperatures, T_e, of the resonant iron nuclei in the specific compounds considered. The ^{56}Fe effective temperature at room temperature was found to be 350(10), 337(16), 309(15), and 358(17) K for $x=0$, 0.083, 0.2, and 0.5, respectively. The results indicate clearly a minimum of the Fe bonding strength in the $Zr(Al_xFe_{1-x})_2$ compounds at $x=0.2$. This minimum correlates nicely with the maximum hydrogen absorption in the above intermetallic system, which may be therefore considered to provide further support for the rule of reverse hydrogen absorption capacity. The conclusions of the present study are utilized to indicate ways for tailoring hydrogen absorption behavior in certain cases.

I. INTRODUCTION

A considerable effort has been spent during the last years[1–6] to examine and improve the experimental feasibility of the nuclear-resonant-photon-scattering (NRPS) technique for investigating the bonding properties of specific metal elements in compounds. The application of this technique to the study of solids in general and metal hydrides in particular was reviewed in Refs. 7 and 8, respectively. The measuring principle is based on an accidental overlap between an incident discrete γ line and a scattering nuclear level, and on a sensitivity of the resonantly scattered radiation to the relevant atomic bonding forces. These forces determine the mean atomic kinetic vibrational energy and therefore the Doppler broadening of the scattering level. The vibrational energy is expressed in terms of the atomic effective temperature, defined and introduced by Lamb[9] under the assumption of harmonic forces and periodicity, and incorporates the zero-point energy contribution. A list of most of the known resonant nuclei, suitable for such a research, is given in Ref. 3. Details about the mathematical analysis of NRPS results may be found in Ref. 10.

In this work we derived the effective temperature of iron in the $Zr(Al_xFe_{1-x})_2$ ($x=0$, 0.083, 0.2, and 0.5) compounds by analyzing the resonant scattering of 8.512-MeV γ rays by the isotope ^{56}Fe. The γ source was generated by the $Cr(n,\gamma)$ reaction. It has been previously found[11] that this scattering process exhibits a significant temperature effect, namely that the scattering intensity drops by approximately 10% when the temperature of the iron scatterer is reduced from 296 to 80 K. This feature makes ^{56}Fe a suitable probe[3] for investigating the iron cohesion properties in different compounds. An evaluation of the effective temperatures required a knowledge of the resonant nuclear parameters— natural radiative widths, energy separation between the incident γ line and the excited nuclear level, and a statistical factor depending on the spins of the resonance and the ground state. As not all of these have been previously determined, we derived in the course of the present work those parameters necessary to accomplish the analysis of the results. Preliminary results, reporting a variation of the resonantly scattered intensity by ^{56}Fe in some of the above compounds, are given in Ref. 6.

The present research was partly undertaken in order to confirm a trend found in $LaAl_xNi_{5-x}$ ($0\le x\le 1.5$) compounds,[5] where the resonantly scattered intensity of 7.646-MeV γ rays by ^{62}Ni revealed a distinct variation of the nickel bonding properties with x. The results indicated that the weakest binding of the Ni atoms occurs in the $LaAl_{0.25}Ni_{4.75}$ intermetallic, followed by a gradual enhancement of the Ni bonding strength with increase of the aluminum content. It was suggested that this bond-

ing strength enhancement is the basis for the decreased hydrogen capacity[12] of the Al-rich $LaAl_xNi_{5-x}$ compounds. Consequently, a rule of reverse capacity[5] (RRC) was formulated. It states that the hydrogen absorption capacity of isostructural intermetallic compounds may decrease with increase of the lattice rigidity and vice versa—it may increase when softening of the lattice occurs. The $LaAl_xNi_{5-x}$ system demonstrates the first, but not the second part of the RRC, as the softening for $x=0.25$ with respect to $x=0$ is not accompanied by an increase of the hydrogen capacity. This behavior is attributed to the high hydrogen capacity of the $LaNi_5$ compound so that any further increase is limited by other factors such as repulsion between close hydrogen atoms. For a more comprehensive demonstration of the RRC, it was suggested[5] to investigate the bonding properties of the $Zr(Al_xFe_{1-x})_2$ system. Its end members, $ZrFe_2$ and $ZrAl_2$ virtually do not absorb hydrogen, while the compounds around $x=0.2$ exhibit a maximum of the hydrogen absorption capacity.[13] It is therefore of interest to determine if a softening in the metal system exists for x values around 0.2 with respect to the surrounding compositions.

II. THEORETICAL REMARKS

The intensity, $C(T,\theta)$, of the scattered radiation at temperature T and angle θ is determined by the overlap between the incident γ line and the excited nuclear level. $C(T,\theta)$ depends on the nuclear parameters Γ, Γ_0, δ, g of the level, on the effective temperatures T_e and T_s of the resonant nucleus, and the (n,γ) source, respectively. In the case of a very thin scatterer, $C(T,\theta)$ is proportional to the effective resonance scattering cross section, $\sigma(T)$, averaged over all the possible γ-ray energies:

$$\sigma(T)=f(\Gamma,\Gamma_0,\delta,g,T_e,T_s)\ . \tag{1}$$

Γ and Γ_0 are the total and the partial ground-state radiative widths, respectively, δ is the energy separation between the incident γ line and the resonance level, g is a statistical factor depending on the spins, J and J_0, of the resonance and the ground states, respectively. In the case of a thick scatterer, thickness corrections should be performed in $C(T,\theta)$ in order to account for the γ-ray absorption. The explicit forms of $C(T,\theta)$ and $\sigma(T)$ are given elsewhere.[10] In many cases it is convenient to utilize experimentally measured ratios R:

$$R(A^c,A^p,T_1,T_2,\theta)=C(A^c,T_1,\theta)/C(A^p,T_2,\theta)\ . \tag{2}$$

A^c and A^p denote an element A in some chemical, c and p, forms, respectively. Equation (2) may be useful in deriving the effective temperature $T_e(A^c,T_1)$ provided all the nuclear parameters and $T_e(A^p,T_2)$ are known. Nuclear parameters may also be determined with the aid of R ratios under certain conditions. The effective temperature T_e is related to the phonon frequency spectrum by

$$\varepsilon\equiv kT_e=\int_0^\infty n(\nu,T)h\nu g(\nu)d\nu\ ,$$
$$n(\nu,T)=\frac{1}{\exp(h\nu/kT)-1}+\frac{1}{2}\ . \tag{3}$$

ε is the mean energy per mode of vibration in the harmonic approximation and $g(\nu)$ is the normalized phonon frequency distribution of a specific atom. The mean energy ε includes also the zero-point energy. In the harmonic approximation the mean kinetic (or potential) energy per vibrational mode equals exactly half of the corresponding total mean energy ε.

III. EXPERIMENTAL DETAILS

A. Target preparation

The $Zr(Al_xFe_{1-x})_2$ ($x=0$, 0.083, 0.2, and 0.5) samples were prepared in an arc furnace under argon atmosphere by melting the weighted fractions of the pure (99.9% or better) metals on a water-cooled copper hearth. The Laves phase cubic structures of these intermetallics were confirmed by x-ray diffraction, and were in good agreement with previously published results.[13,14] Samples, weighing about 200 g, were crushed into powder and introduced into specially designed plastic holders of 6-cm internal diameter. Measurements were always performed in pairs. One of the constituents of the pair consisted of an intermetallic compound alone. The other member of the pair consisted of another intermetallic compound, containing the same amount of Fe, to which elemental zirconium and aluminum powders have been added so that the two members of the pair were identical in composition by weight. Special care was also taken to form homogeneously distributed specimens. $ZrFe_2$ was the reference sample for the two $Zr(Al_xFe_{1-x})_2$ ($x=0.083$, 0.2) specimens. $Zr(Al_{0.2}Fe_{0.8})_2$ and $Zr(Al_{0.5}Fe_{0.5})_2$ constituted another pair as it was easier to achieve homogeneity for closer compositions. Using such targets, all corrections due to atomic attenuation and multiple photon scattering within the sample are eliminated. Another sample holder was filled with pure Zr, Al, and Mn powders of comparable weights for background subtraction purposes. We were able to keep the geometrical thicknesses of the different samples nearly identical (about 18 mm) by applying moderate pressures on the metal powders when necessary. Additional comparison was done between $ZrFe_2$ and a mechanical mixture of pure zirconium and iron powders. In this case we added organic powder to expand the $ZrFe_2$ sample and thus obtain equal thicknesses of the two specimens.

B. γ resonant scattering setup

The targets were placed in a photon beam obtained from the $Cr(n,\gamma)$ reaction utilizing thermal neutrons from the Israel Research Reactor-2. The γ source consisted of several chromium discs inserted along a tangential beam port near the reactor core. The incident γ beam is collimated along a distance of several meters and

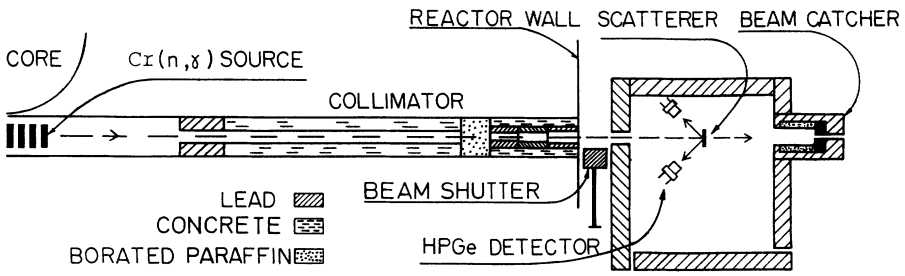

FIG. 1. Schematic representation of the experimental setup used in the present work.

then impinged upon the target situated in an experimental lead chamber. The neutron flux of about 2×10^{13} neutrons $cm^{-2}sec^{-3}$ yields an intensity on the target of about 10^5 photons $cm^{-2}sec^{-1}$ per strong single γ line. A more detailed description of the measuring facilities utilized for the γ-ray resonance scattering experiments performed at the Nuclear Research Center-Negev may be found in Refs. 10 and 15. Figure 1 presents a schematic description of the experimental facility.

The scattered photons from the targets were detected by a 130-cm^3 HPGe detector of 27% efficiency, and a smaller 40-cm^3 Ge detector, both placed at backward angles with respect to the incident γ beam. The scattered intensities in each pair of targets were compared by interchanging samples at approximately constant time intervals. Care was taken to ensure that the samples were exactly in the same position with respect to the incident photon beam. In addition, the homogeneity of the targets was monitored by rotating them subsequently through 90° in a plane perpendicular to the impinging photons. Background measurements were carried out utilizing the Zr-Al-Mn mixture.

In order to determine some of the nuclear parameters of ^{56}Fe, a similar setup was utilized to compare the resonant scattering intensities of massive iron and copper disc targets. They scatter resonantly neighboring (see below) γ lines from the Cr(n,γ) source. The 8.512-MeV scattered photon intensity by ^{56}Fe was also measured at target temperatures of 12, 296, 573, and 673 K. The cooling was achieved by utilizing a cryostat, and heating was performed by an electric current flow through a resistance wire located on the target circumference.

IV. EXPERIMENTAL RESULTS AND DISCUSSION

A. Determination of the nuclear parameters of the ^{56}Fe 8.512-MeV level

Some of the nuclear parameters, namely the branching ratio Γ_0/Γ and the statistical factor g of the ^{56}Fe 8.512-MeV level are known from a previous study.[11] The knowledge of two more parameters, namely Γ and δ, was necessary for quantifying our experimental results in terms of effective temperatures. Two independent experiments were therefore carried out. In one of them we determined the effective elastic cross section for the Cr(n,γ)-^{56}Fe 8.512-MeV resonance scattering process by comparing its intensity to that of the Cr(n,γ)-^{65}Cu 8.484-MeV resonance event. The copper effective scattering cross section is known from a previous work[16] to be (205±26) mb. The comparison yielded

$$\sigma(296\,\mathrm{K})=(0.66\pm0.22)\ \mathrm{mb}$$

for the Cr(n,γ)-^{56}Fe resonance scattering. The result was obtained after taking into account and eliminating the factor of atomic self-absorption. The second experiment provided measured intensity ratios of the type given in Eq. (2) for pure iron at three temperature sets. The reference temperature in all three sets was always 296 K (room temperature), and the second temperature was set either to 12, 573, or 673 K. Table I presents the measured $R(\mathrm{Fe},T_1,296\ \mathrm{K},135°)$ ratios. Fe stands for pure iron and for brevity it appears only once in R. Background was subtracted after measuring nonresonant scattered radiation by a Co target.

The total radiation width Γ of the 8.512-MeV ^{56}Fe nuclear level and its energy displacement δ from the corresponding incident γ line of the Cr(n,γ) source were determined by plotting the experimentally derived scattering cross section σ and temperature effects R in the Γ-δ plane. Figure 2 presents such a plot for $\sigma(296\ \mathrm{K})=0.66$ mb and $R(\mathrm{Fe},673\ \mathrm{K},296\ \mathrm{K},135°)=1.522$. The σ and R curves in the figure are the geometrical loci of Γ and δ pairs yielding the given 0.66 mb and 1.522 values, respectively. Figure 2 clearly indicates the existence of only one intersection point between the two curves. Similar intersection points were obtained with the two additional temperature effect values (see Table I). These intersections determine the Γ and δ values of the 8.512-MeV ^{56}Fe level:

$$\Gamma=(0.67\pm0.10)\ \mathrm{eV},\quad \delta=(44\pm1)\ \mathrm{eV}\ .$$

Previously derived parameters[11] were utilized for obtaining these plots, namely a branching ratio $\Gamma_0/\Gamma=0.3$, and a statistical factor $g=(2J+1)/(2J_0+1)=3$ for $J=1$ and $J_0=0$. The source effective temperature T_S was approximately 440 K. The effective temperatures of the resonant

TABLE I. Measured (±0.015) intensity ratios $R(\mathrm{Fe},T_1,296\ \mathrm{K},135°)$ for 8.512-MeV γ radiation from Cr(n,γ) source, scattered resonantly by ^{56}Fe in a pure iron target of 0.8-cm thickness.

T_1 (K)	10	573	673
$R(\mathrm{Fe},T_1,296\ \mathrm{K},135°)$	0.895	1.323	1.522

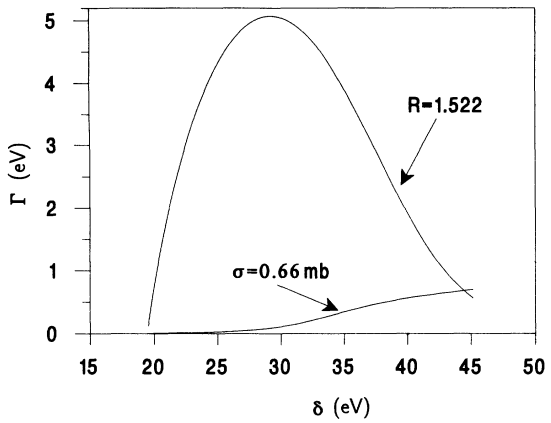

FIG. 2. Determination of the total radiation width Γ of the 8.512-MeV nuclear ^{56}Fe level, and the energy distance δ of this level to the incident γ line from the Cr(n,γ) source. The intersection of the R(Fe, 673 K, 296 K, 135°)=1.522 and σ(296 K)=0.66 mb curves (see also text) in the Γ-δ plane yields the desired values.

scatterer at the different temperatures were estimated by utilizing the Debye approximation $g(\nu)=3\nu^2/\nu_D^3$, thus reducing Eq. (3) to

$$T_e=\frac{3}{8}\Theta_D+3T\left[\frac{T}{\Theta_D}\right]^3\int_0^{\Theta_D/T}\frac{x^3}{\exp x-1}dx\ . \quad (4)$$

It should be stressed that the intersection points (Γ,δ) were almost not sensitive to the choice of the Debye temperature Θ_D of iron. A variation of Θ_D between 390 and 480 K did not influence significantly our results. The determination of Γ and δ may therefore be regarded as independent of the effective temperature of the scatterer in the present case. This behavior is attributed to the large δ value in the particular case studied here.

B. Determination of T_e of iron in the Zr(Al$_x$Fe$_{1-x}$)$_2$ compounds (x =0, 0.083, 0.2, 0.5)

The scattered intensity I from the various resonant targets was obtained by integrating over all counts in the energy range E=7.0–8.6 MeV. The results were analyzed using the measured ratio R defined in Eq. (2):

$$R_{ij}\equiv R(\mathrm{Fe}^i,\mathrm{Fe}^j,296\ \mathrm{K},296\ \mathrm{K},135°)$$
$$=(I_i-B)/(I_j-B)\ , \quad (5)$$

where i and j denote different compounds or pure iron. The same background B appears in the nominator and denominator, as the two scattering targets contained exactly the same quantities of the elements (see above). These experimental measures guarantee that the R values reflect directly the relative bonding strength of the iron atoms in states i and j, as this is the only difference between the two targets. A detailed calculation was made to check the influence of relatively small variations in the thickness of the various targets on the resonantly scattered intensity for the particular scatterer-detector configuration. It was found that a 10% variation in the thickness, while the overall material quantities are kept constant, causes approximately 0.1% variation in the corresponding resonant scattered intensities (RSI). This is much less than the observed effects or the experimental errors reported below. On the other hand, it appeared that a significant RSI reduction of about 1% was caused by the blank organic material added to compensate the large volume differences for the $ZrFe_2$-Zr+2Fe pair. A corresponding correction was done in this case. Table II presents our measured resonant scattered intensity ratios R. The experimental errors were determined by considering the ratio of the dependent variables in Eq. (5).

Our measurements enable us to evaluate the effective temperatures T_e of the resonant nuclei in the specific compounds considered. Equations (1) and (2) were employed for this evaluation by utilizing the measured R ratios, the known nuclear parameters, Γ, Γ_0, δ, J, J_0, and the T_e value of pure iron. The latter is obtained from Eq. (3) by substituting into it the phonon frequency spectrum of elemental Fe, derived from neutron inelastic data.[17] The detailed expressions used in Eqs. (1) and (2) may be found in Ref. 10. The calculated T_e values are also listed in Table II and plotted in Fig. 4. Additional experimental errors are introduced by normalizing all the figures to the same reference point, namely pure iron. The results, presented in Figs. 3 and 4 and Table II, indicate a significant decrease of the iron cohesion in the Zr(Al$_x$Fe$_{1-x}$)$_2$ system with the increase of the aluminum content from x =0 to x =0.2. A further increase of the Al composition to x =0.5 causes a rise in the Fe bonding strength. This behavior is demonstrated by the T_e sequence 350 K→309 K→358 K, and indicates a good agreement with the prediction of the RRC, i.e., the increase of the bonding strength for all x values with respect to x =0.2 correlates nicely with the large decrease of the hydrogen capacity in Zr(Al$_x$Fe$_{1-x}$)$_2$ from a maximum of 3 H atoms in Zr(Al$_{0.2}$Fe$_{0.8}$)$_2$ to 0.5 and 1.25 H atoms in $ZrFe_2$ and Zr(Al$_{0.5}$Fe$_{0.5}$)$_2$, respectively.[13,18]

TABLE II. Measured resonant scattered intensity ratios, R [see Eqs. (2) and (5)], of the 8.512-MeV γ line at room temperature, normalized to iron in $ZrFe_2$ for thicknesses 1.8–3.6 (g Fe)/cm^2. The Zr(Al$_x$Fe$_{1-x}$)$_2$ compounds are characterized by their x values. The corresponding effective temperatures T_e are also presented.

Sample (x)	Fe	0	0.083	0.2	0.5
R	0.983±0.008	1	0.990±0.007	0.972±0.007	1.006±0.01
T_e (K)	327	350±10	337±16	309±15	358±17

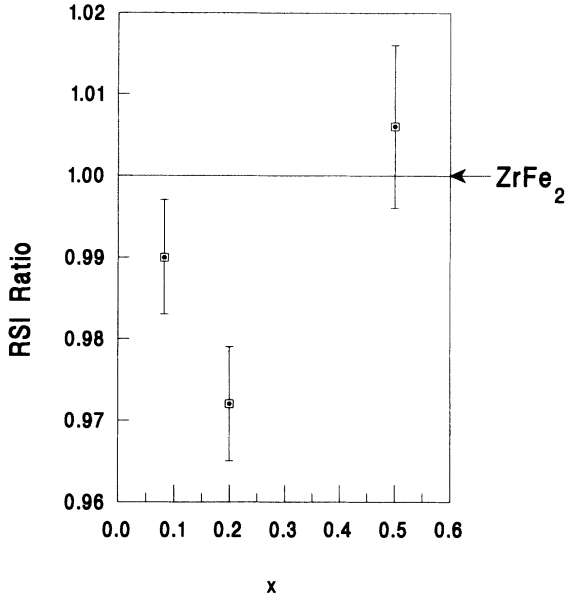

FIG. 3. Variation of the 8.512-MeV resonant scattered intensity (RSI) by ^{56}Fe in the different $Zr(Al_xFe_{1-x})_2$ compounds, $x=0$, 0.083, 0.2, 0.5, normalized to $ZrFe_2$.

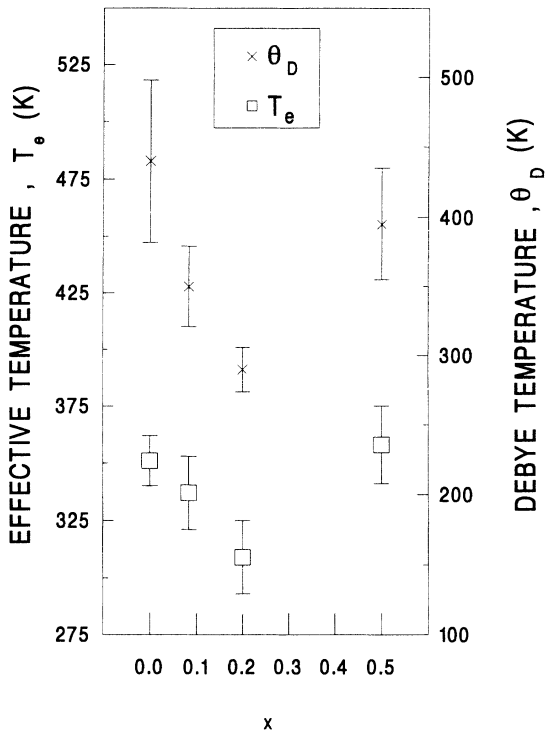

FIG. 4. Effective temperatures T_e in the $Zr(Al_xFe_{1-x})_2$ compounds, $x=0$, 0.083, 0.2, 0.5, derived in the present work and the corresponding Θ_D values obtained from a Mössbauer experiment (Ref. 19).

C. Comparison with Mössbauer and other experiments

Another important result of the present work is that we were able for the first time to compare NRPS results with those of another microscopic technique, as the Mössbauer effect was utilized to study the iron cohesion properties in the $Zr(Al_xFe_{1-x})_2$ system by way of the recoilless absorption in ^{57}Fe.[19] Debye temperatures were derived by analyzing recoil free fraction ratios at three temperature sets. It should be stressed that the effective temperatures T_e obtained in the present work, are less model dependent than the Debye temperatures Θ_D evaluated from the Mössbauer experiment. The Debye model was not applied for deriving T_e, but has been obviously used in the relevant Mössbauer analysis. Nevertheless, both T_e and Θ_D reflect the iron bonding strength in the compounds studied. Figure 4 exhibits also Θ_D Mössbauer values, derived from one temperature set,[19] for those intermetallics investigated in the present work. The T_e and Θ_D trends, demonstrated in Fig. 4, reveal a very good qualitative agreement between the results of the two techniques. The minimum of the iron bonding strength at $x=0.2$ is indicated in both experiments. We stress once again that NRPS results for specific metal cohesion properties in compounds are directly compared with another technique, and supported by it. On the contrary, no minimum in the cohesion properties of the $Zr(Al_xFe_{1-x})_2$ was observed macroscopically by measuring the heats of formation[20] of this system. This emphasizes the importance and the ability of the NRPS technique to provide a unique microscopic insight in certain compounds.

To the best of our knowledge the observed minimum of the atomic bonding properties is the only prominent correlation with the measured maximum of the hydrogen absorption capacity in the $Zr(Al_xFe_{1-x})_2$ system. These Laves-phase compounds exhibit a smooth transition from the cubic $MgCu_2$-type to the hexagonal $MgZn_2$-type structure at $x=0.25$, i.e., the two structures are closely related to each other. Their lattice cell volume per formula unit, interatomic distances and hence the size of the interstitial sites, available for hydrogen occupation, change continuously and monotonically throughout the whole x range between 0 and 1. We cannot exclude the possibility of stabilizing the metal lattice by the hexagonal structure, but there is no reasonable evidence for a direct correlation between the cubic or the hexagonal configuration and the H absorption properties. The independence of the hydrogen absorption capacity on the above cubic-hexagonal transition is probably best demonstrated by the identical hydrogen absorption in the two allotropic Laves-phase forms of $ZrCr_2$.[21] It may be noted in passing that a good phenomenological fit has been obtained for the hydrogen capacity of Zr-based Laves-phase pseudobinary systems[13,22] by considering clusters composed by a Zr atom and its twelve nearest neighbors. This indicates the importance of short-range neighboring effects which probably influence the atomic bonding strengths. It is worthwhile to mention also the probable randomization of the Al and Fe positions in the lattice of $Zr(Al_xFe_{1-x})_2$ implied by the measured linear relationship of the relevant enthalpies of formation over most of the range of x.[20] Additional support for the significance of our results was recently found in a work[23] stating that the hydrogenation behavior of the $LaAl_xNi_{5-x}$

($0 \leq x \leq 1.5$) compounds, all of which crystallize in the hexagonal $CaCu_5$-type structure,[12] is different for x greater or smaller than 0.25. This is exactly the composition at which a minimum in the Ni bonding strength was previously found for this system.[5]

V. SUMMARY

In summary, we found in this work a distinct variation of the iron bonding strength in $Zr(Al_xFe_{1-x})_2$ ($0 \leq x \leq 0.5$) compounds by utilizing NRPS from ^{56}Fe. This variation was quantified in terms of effective temperatures. The observed behavior of the T_e in the above system closely resembles previous results on the bonding strength of Ni in $LaAl_xNi_{5-x}$ ($0 \leq x \leq 1.5$) compounds. We thus regard the present work as a confirmation and evidence that the observed effects are not an isolated or fortuitous phenomenon. It is consequently suggested that systems, such as $ThAl_xNi_{5-x}$,[24] $Er(Co_xFe_{1-x})_2$,[25] and $Zr(Al_xCo_{1-x})_2$,[13] exhibiting maximum in their hydrogen absorption capacity, would reveal similar bonding properties as the currently studied compounds. The present research may have important consequences in indicating ways for tailoring initiation or inhibition of hydrogen absorption in certain cases. For example, we believe that softening the bonding strength of one or more constituents in the very stable,[26] hydrogen-inert intermetallics $ZrPd_2$ (Refs. 27 and 28) and UPd_3 (Ref. 29) by proper alloying will cause them to absorb hydrogen.

ACKNOWLEDGMENT

This research was supported by the Basic Research Foundation administered by the Israel Academy of Sciences and Humanities.

[1]R. Moreh, O. Shahal, and I. Jacob, Nucl. Phys. **A228**, 77 (1974).
[2]I. Jacob, M. H. Mintz, O. Shahal, and A. Wolf, Phys. Lett. A **32**, 45 (1981).
[3]I. Jacob, A. Wolf, O. Shahal, and R. Moreh, Phys. Rev. B **33**, 5042 (1986).
[4]I. Jacob, R. Moreh, O. Shahal, and A. Wolf, Phys. Rev. B **35**, 8 (1987).
[5]I. Jacob, R. Moreh, O. Shahal, A. Wolf, and Z. Gavra, Phys. Rev. B **38**, 7806 (1988).
[6]I. Jacob, A. Israel, R. Moreh, and A. Wolf, Z. Phys. Chem. **181**, 55 (1993).
[7]R. Moreh, Nucl. Instrum. Methods **166**, 45 (1979).
[8]M. H. Mintz, I. Jacob, and D. Shaltiel, in *Hydrogen in Intermetallic Compounds 2,* edited by L. Schlapbach, Topics in Applied Physics, Vol. 67 (Springer-Verlag, Berlin, 1992), p. 285.
[9]W. E. Lamb, Jr., Phys. Rev. **55**, 190 (1939).
[10]R. Moreh, S. Shlomo, and A. Wolf, Phys. Rev. C **2**, 1144 (1970).
[11]R. Moreh and O. Shahal (unpublished).
[12]M. H. Mendelsohn, M. D. Gruen, and A. E. Dwight, Nature (London) **269**, 45 (1977).
[13]I. Jacob and D. Shaltiel, Solid State Commun. **27**, 175 (1978).
[14]Y. Muraoka, M. Shiga, and Y. Nakamura, Phys. Status Solidi A **42**, 369 (1977).
[15]A. Wolf, R. Moreh, and O. Shahal, Nucl. Phys. **A227**, 373 (1974).
[16]R. Moreh, O. Shahal, and J. Tennenbaum (unpublished).
[17]H. Schober and P. H. Dederichs, in *Phonon States of Elements, Electron States and Fermi Surfaces of Alloys,* edited by K. H. Hellwege and K. H. Olsen, Landolt-Börnstein, New Series, Group III, Vol. 13a (Springer, Berlin, 1981).
[18]A. Stern (private communication).
[19]I. Nowik, I. Jacob, and R. Moreh, Phys. Rev. B **47**, 723 (1993); I. Jacob, I. Nowik, and R. Moreh, Z. Phys. Chem. **181**, 61 (1993).
[20]R. Klein, I. Jacob, P. A. G. O'Hare, and R. Goldberg, J. Chem. Thermod. (to be published).
[21]I. Jacob, Ph.D. thesis (in Hebrew), Hebrew University of Jerusalem, Jerusalem, 1980.
[22]I. Jacob, D. Shaltiel, D. Davidov, and I. Miloslavski, Solid State Commun. **22**, 669 (1977).
[23]E. Akiba, H. Hayakawa, Y. Ishido, K. Nomura, S. Shin, and T. Minesawa, MRS Mtg. Adv. Mats. **2**, 39 (1989).
[24]T. Takeshita and W. E. Wallace, J. Less-Common Met. **55**, 61 (1977).
[25]D. M. Gualtieri and W. E. Wallace, J. Less-Common Met. **55**, 53 (1977).
[26]F. R. de Boer, R. Boom, W. C. M. Mattens, A. R. Miedema, and A. K. Niessen, *Cohesion in Metals* (North-Holland, Amsterdam, 1989).
[27]A. J. Maeland and G. G. Libovitz, J. Less-Common Met. **74**, 295 (1980).
[28]L. Schlapbach, S. Hüffner, S. Büchler, and T. Riesterer, J. Less-Common Met. **130**, 301 (1987).
[29]R. Feenstra, D. G. de Grot, R. Griessen, J. P. Burger, and A. Menovski, J. Less-Common Met. **130**, 375 (1987).